Electronic Supplementary Material (ESI) for Dalton Transactions

Supporting Information

Dual channel selective fluorescence detection of Al(III) and PPi in aqueous media with '*off-on-off*' switch which mimics Molecular logic gating (INHIBIT and EXOR gate) Interpretations

Shyamaprosad Goswami*, Abhishek Manna, Sima Paul, Krishnendu Aich, Avijit K. Das and Shampa Chakroborty

Department of Chemistry, Bengal Engineering and Science University, Shibpur, Howrah 711103, West Bengal, India E-mail: spgoswamical@yahoo.com; Fax: +91-3326682916.

CONTENTS

1. Job Plot by fluorescence method:

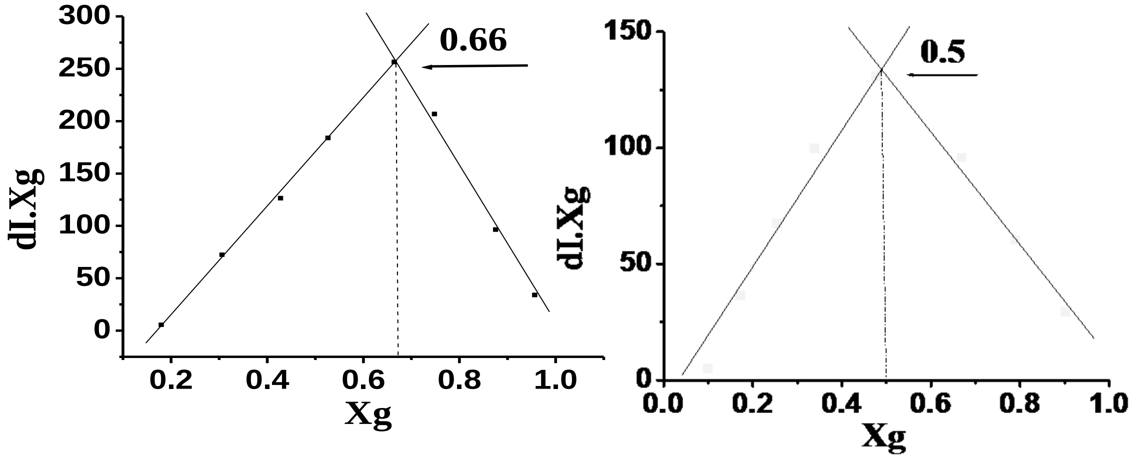

Figure S1: Job plot diagram of receptor i.e. ISH with Al^{3+} (left) and PPi (right) (where X_g is the mole fraction of the Al^{3+} and PPi respectively and dI indicates the change of Fl.Intensity).

2. Effect of pH:

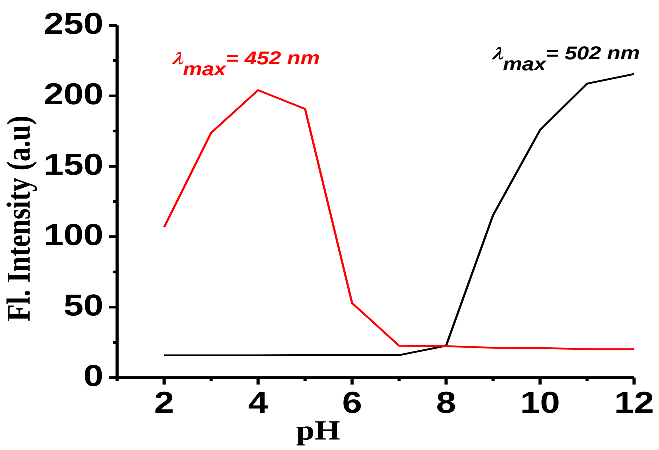

Figure S2: pH titration curve of ISH (C=1X10^{-5} M) in fluorescence spectroscopy, pH is adjusted with $HClO_4$ and NaOH.

3. Determination of fluorescence quantum yield:

Here, the quantum yield φ was measured by using the following equation,

$\varphi_x = \varphi_s (F_x / F_s)(A_s / A_x)(n_x^2/ n_s^2)$
Where,
X & S indicate the unknown and standard solution respectively, φ = quantum yield,
F = area under the emission curve, A = absorbance at the excitation wave length,
n = index of refraction of the solvent. Here φ measurements were performed using anthracene in ethanol as standard [φ = 0.27] (error ~ 10%).
The quantum yield of **ISH** itself is 0.00328 which remarkably changed to 0.8296 (around 252 fold enhancements) on the formation of a complex with Al^{3+} metal ion and 0.4123 (around 125 fold enhancements) due to binding with PPi respectively.

4. Determination of the association constants:

The spectra of these solutions were recorded by means of fluorescence methods. Binding constant was calculated according to the Benesi-Hildebrand equation. K_a was calculated following the equation stated below.

$$1/(F\text{-}Fo) = 1/\{K(Fmax–Fo)\ [Al^{3+}]_n\} + 1/[Fmax\text{-}Fo]$$

$$1/(F\text{-}Fo) = 1/\{K(Fmax–Fo)\ [P_2O_7^{4-}]_n\} + 1/[Fmax\text{-}Fo]$$

Here Fo is the fluorescence of receptor in the absence of guest, F is the fluorescence recorded in the presence of added guest, Fmax is fluorescence in presence of added $[Al^{3+}]$max and $[P_2O_7^{4-}]$max, K is the association constant (M^{-1}). The association constant (K_a) could be determined from the slope of the straight line of the plot of 1/(F-Fo) against $1/[Al^{3+}]_n$ and $1/[P_2O_7^{4-}]_n$ respectively. The association constant (K_a) as determined by fluorescence titration method for sensor with Al^{3+} and PPi is found to be 1.08 x 10^5 M^{-1} and 9.7 x 10^4 M^{-1} respectively.

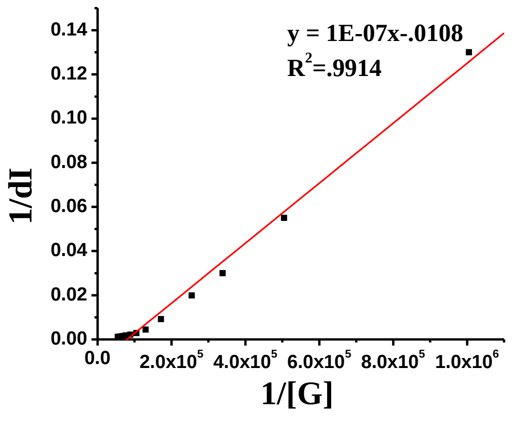

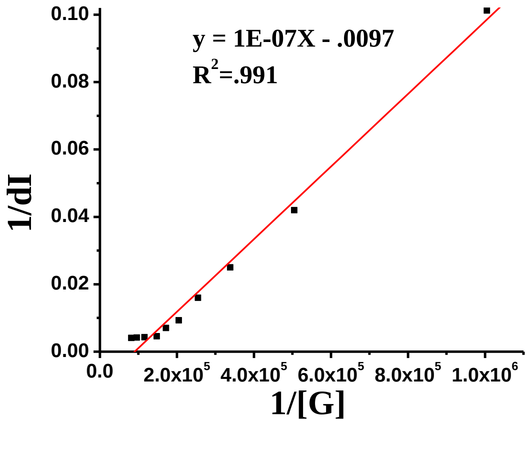

Figure S3: Benesi-Hildebrand plot.

Determination of the association constant of ISH with Al^{3+} by nonlinear least-squares analysis:

The association constant K_{11} and K_{12} were determined by nonlinear least-squares analysis of Y versus c_M using the following equation[1].

$$Y = \frac{Y_0 + c_M \Phi K_{11}[M] + Y_{lim} \beta_{21}[M]^2}{1 + K_{11}[M] + \beta_{21}[M]^2}$$

Where $\beta_{21} = K_{11}K_{21}$, $[M] \approx c_M$ is Al^{3+} ion concentration, Y_0 or Y is integrated emission in the absence or presence of Al^{3+} ion, Φ is the quantum yield of the sensor-Al^{3+} complex in 1:1 stoichiometry.

Table. Association constants of ISH with Al^{3+}

Entry	$K_{11}/M^{-1}(10^4)$	$K_{12}/M^{-1}(10^4)$
ISH / Al^{3+}	5.366	17.653

5. Calculation of the detection limit:

The detection limit DL of **ISH** for Al(III) and PPi was determined from the following equation[2]:

DL = K* Sb1/S

Where K = 2 or 3 (we take 2 in this case); Sb1 is the standard deviation of the blank solution; S is the slope of the calibration curve.

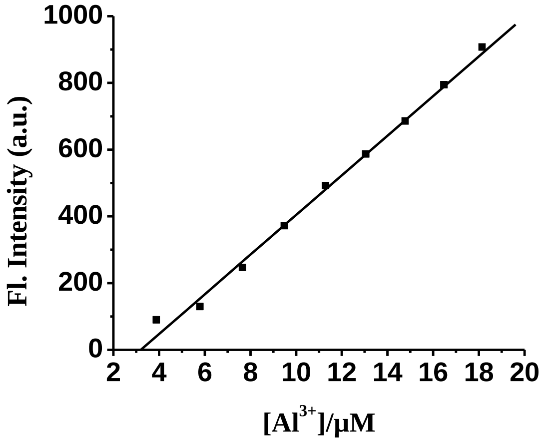

A	**-190.20355**	**20.10059**
B	**59.43123**	**1.65893**

R	SD	N	P
0.99728	**22.90228**	**9**	**<0.0001**

Figure S4: Fl. Intensity vs. [Al^{3+}] plot.

From the Fl. intensity vs. [Al^{3+}] graph, we get slope = 59.43123, and Sb1 value is 22.90228. Thus using the formula, we get the Detection Limit = 0.77 μM i.e. ISH can detect Al^{3+} ion in this minimum concentration.

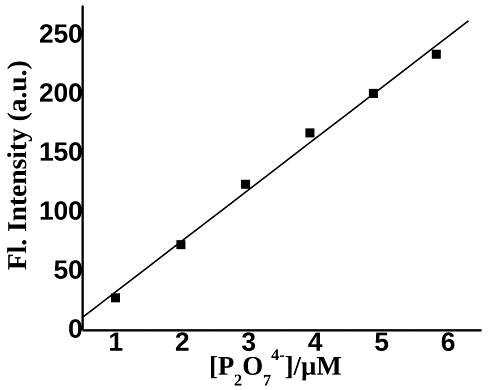

A	**-10.51144**	**6.57914**
B	**43.22648**	**1.73021**

R	SD	N	P
0.99681	**6.99218**	**6**	**<0.0001**

Figure S5: Fl. Intensity vs. [PPi] plot.

From the Fl. Intensity vs. [$P_2O_7^{4-}$] graph we get slope = 43.226, and Sb1 value is 45.572. Thus using the formula we get the Detection Limit = 1.71 μM i.e. ISH can detect $P_2O_7^{4-}$ ion in this minimum concentration.

6. [1]H NMR, [13]C NMR and ESI MS spectra:

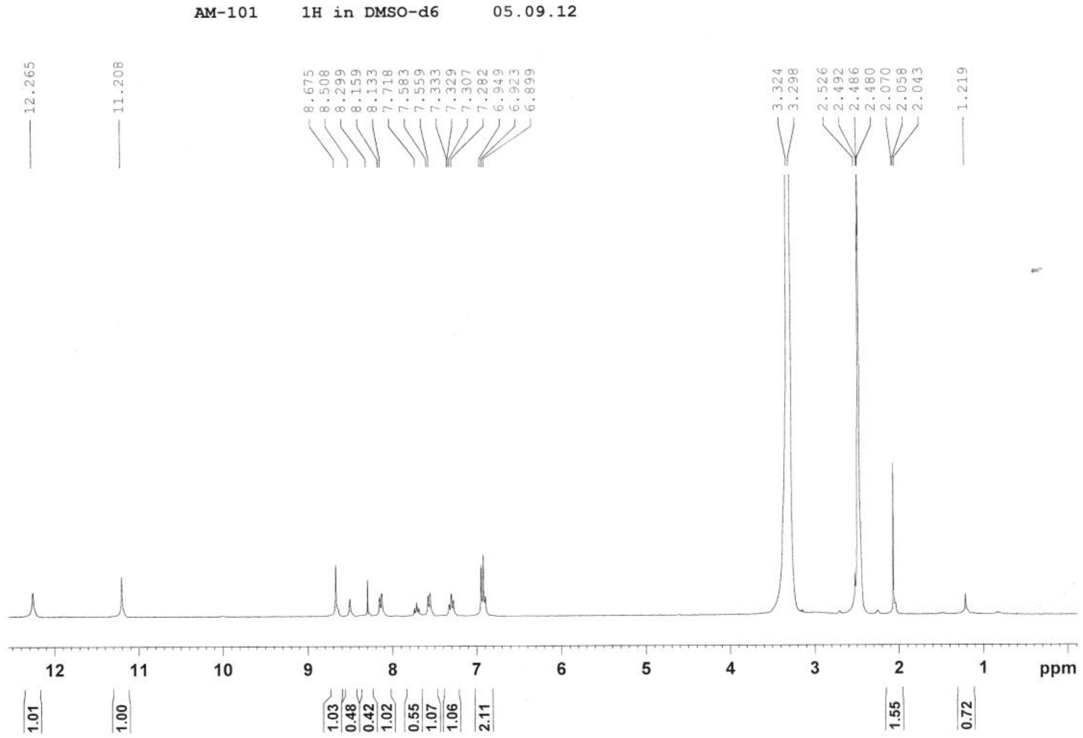

Figure S6: ^{1}H-NMR spectra of ISH.

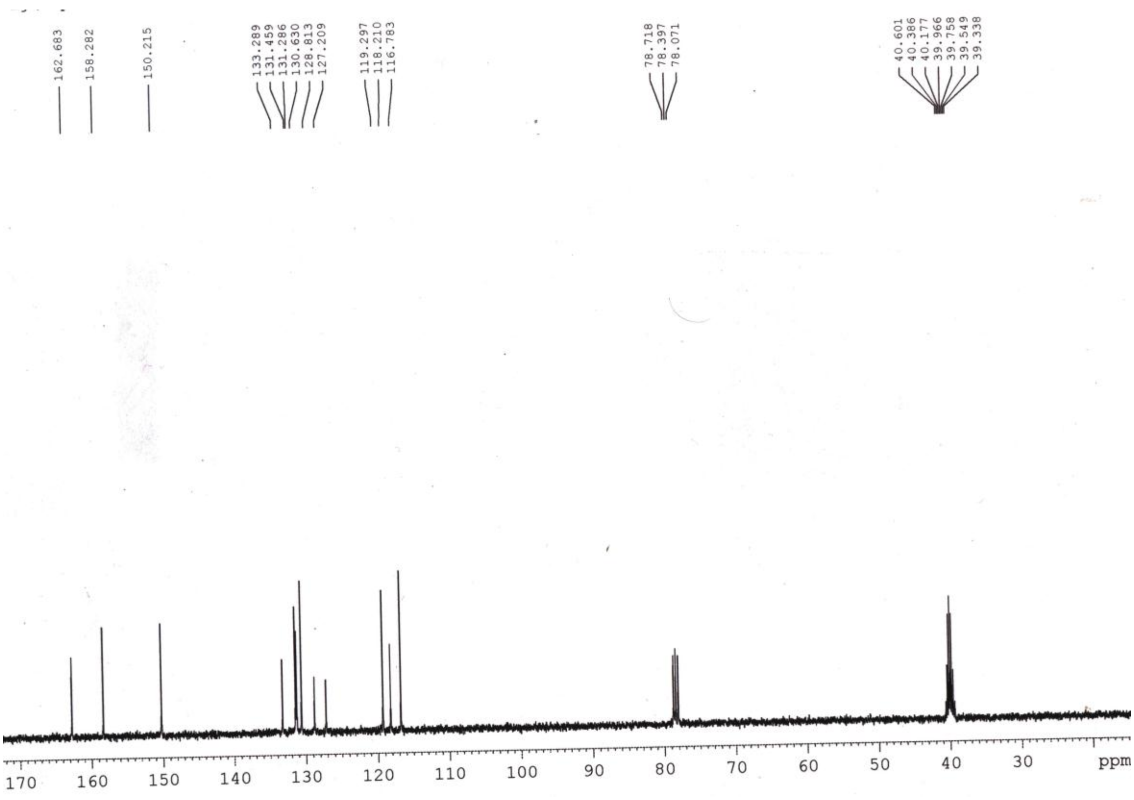

Figure S7: ^{13}C-NMR spectra of ISH.

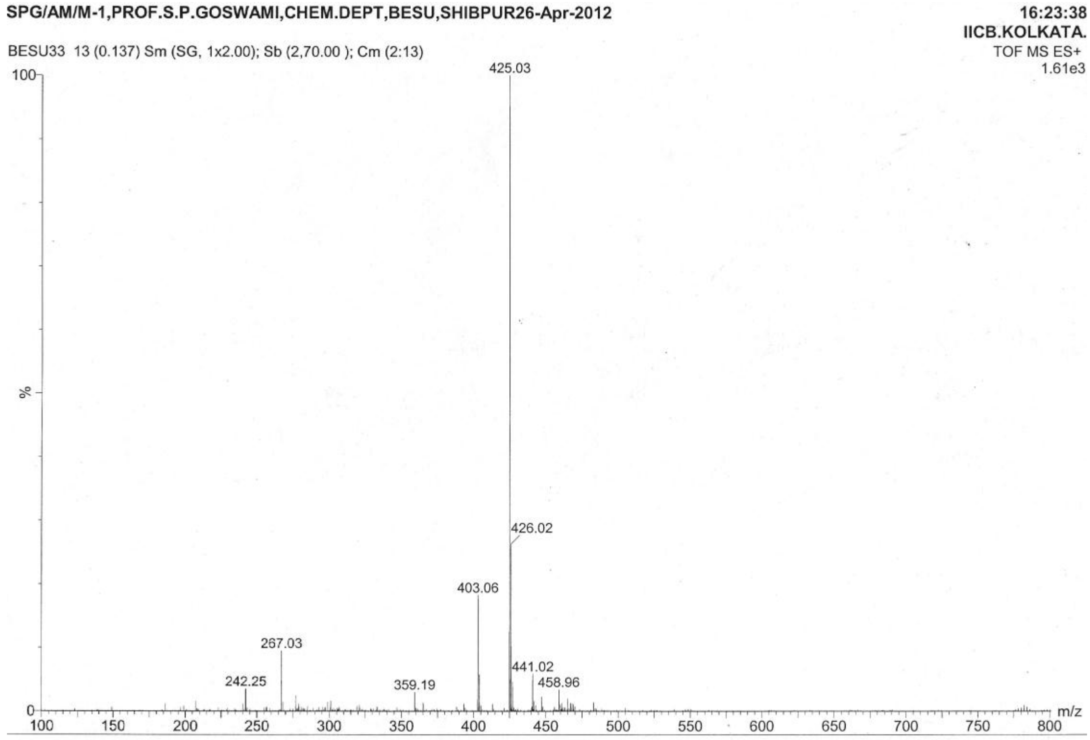

Figure S8: ESI-MS spectra of ISH.

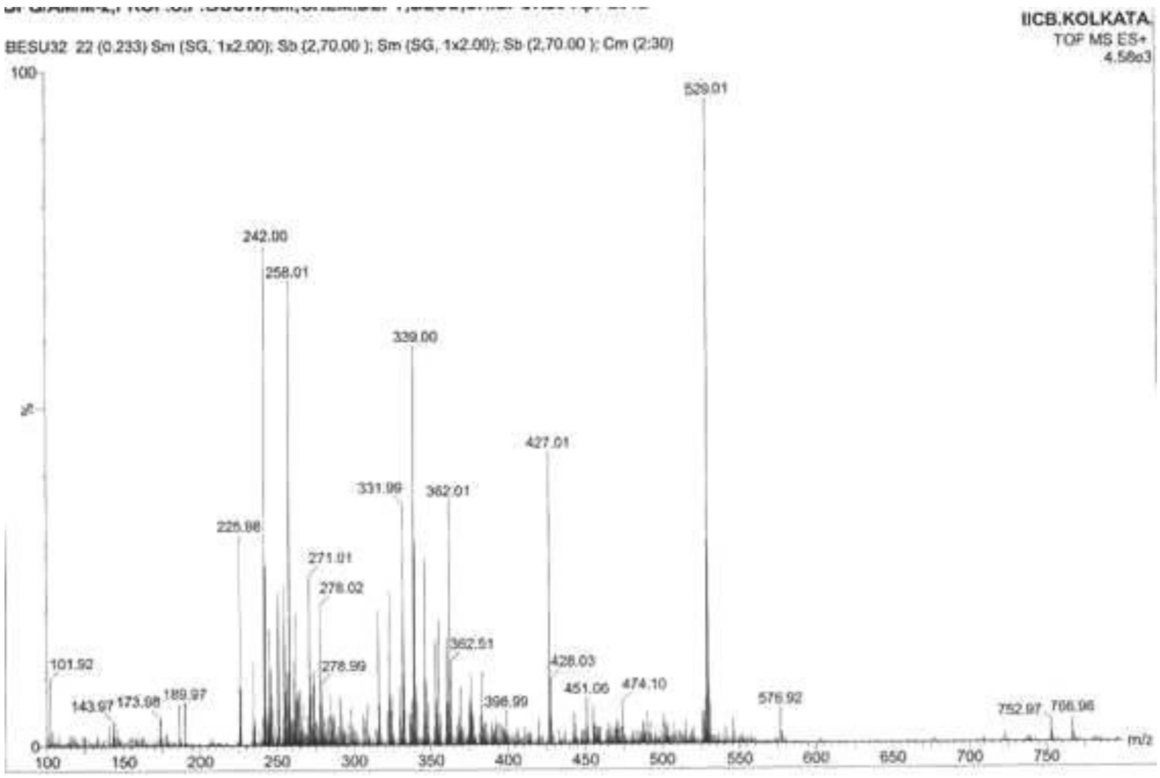

Figure S9: ESI-MS spectra of ISH-Al^{3+} complex.

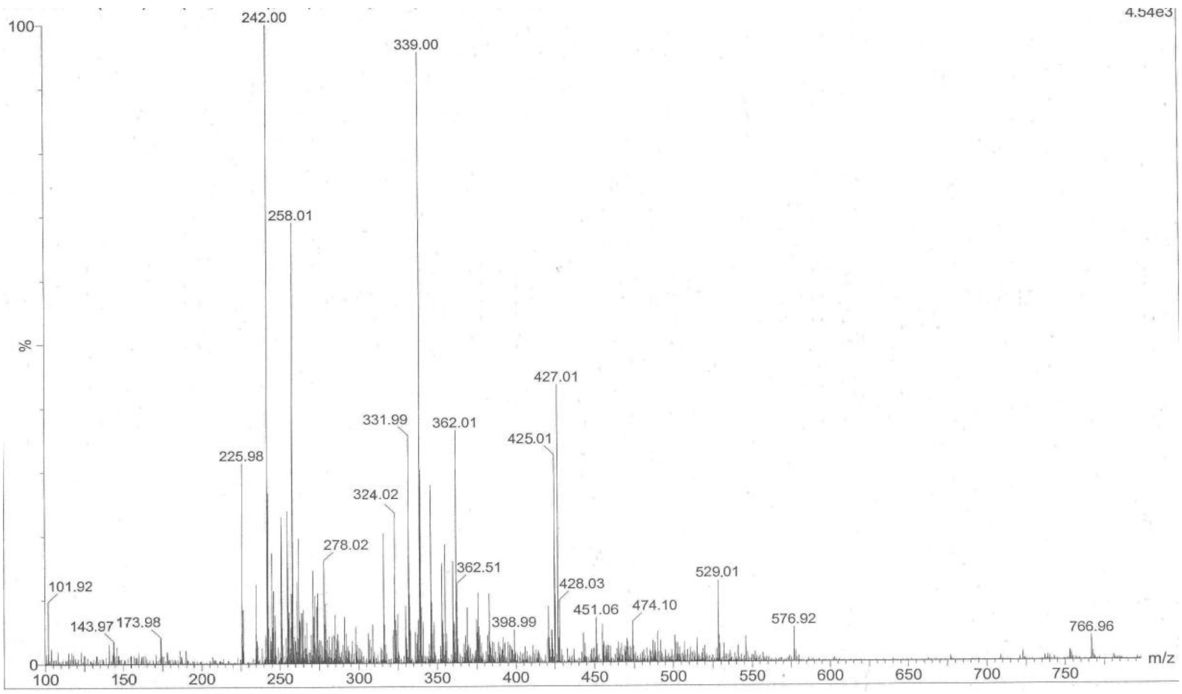

Figure S10: ESI-MS spectra of PPi added ISH-Al^{3+} complex.

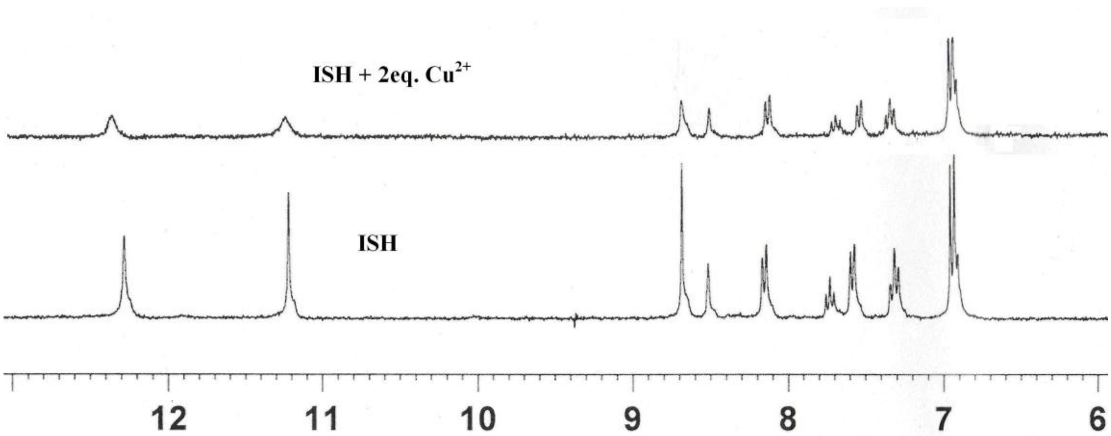

Figure S11: Partial ^{1}H-NMR spectra of ISH with addition of 2eq. Cu^{2+} in d_6-DMSO.

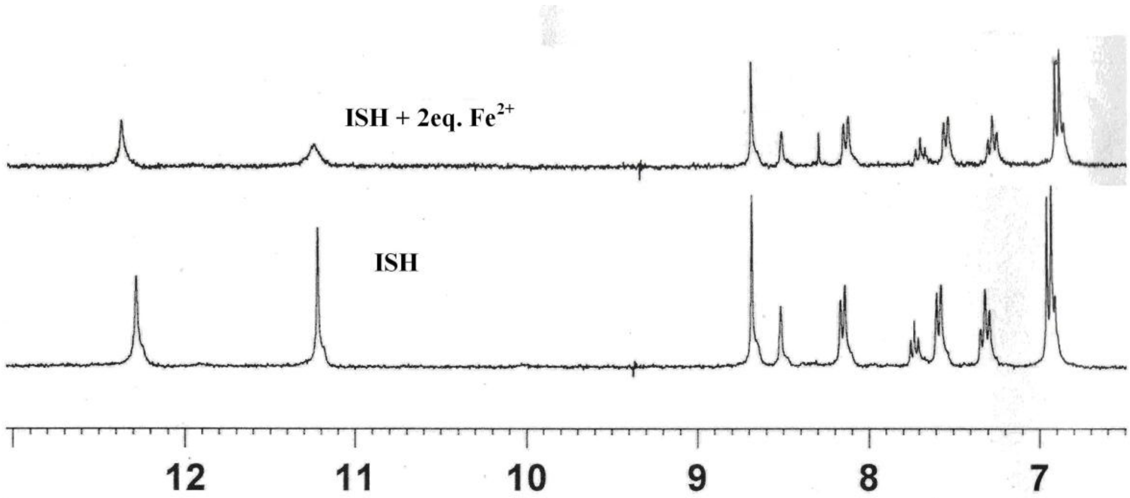

Figure S12: Partial ^{1}H-NMR spectra of ISH with addition of 2eq. Fe^{2+} in d_6-DMSO.

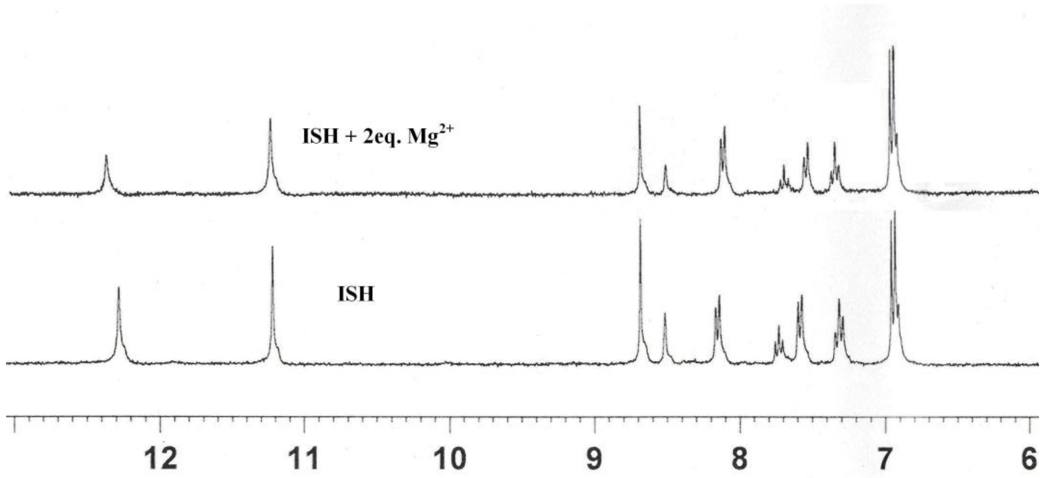

Figure S13: Partial ^{1}H-NMR spectra of ISH with addition of 2eq. Mg^{2+} in d_6-DMSO.

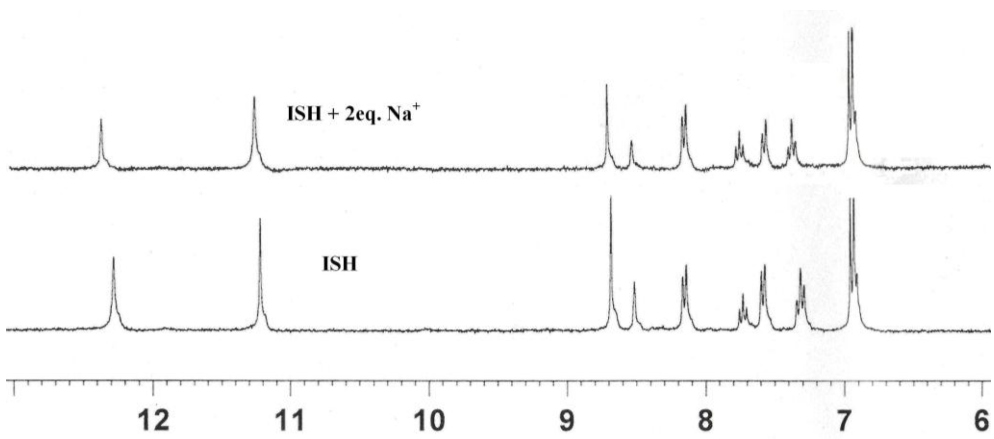

Figure S14: Partial ^{1}H-NMR spectra of ISH with addition of 2eq. Na^{+} in d_6-DMSO.

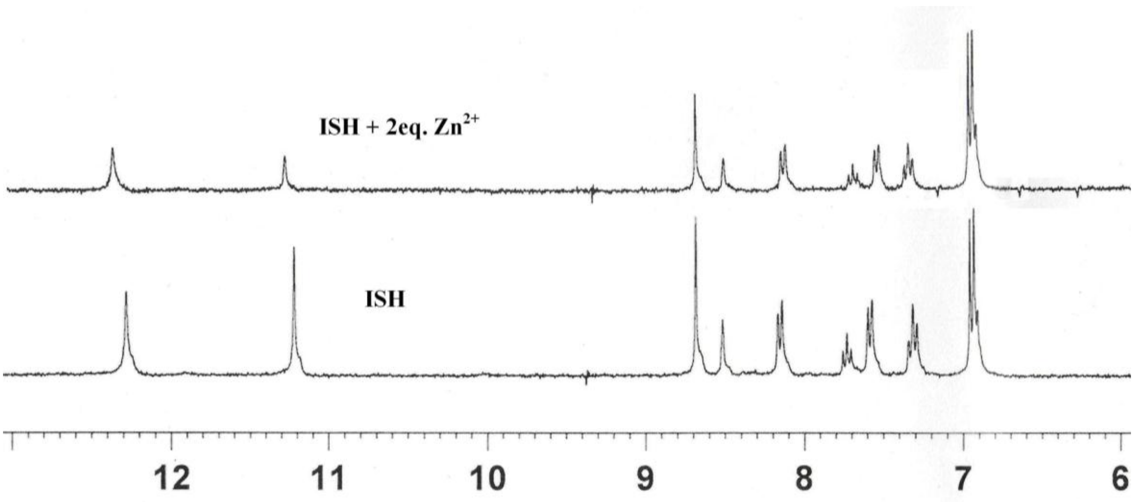

Figure S15: Partial ^{1}H-NMR spectra of ISH with addition of 2eq. Zn^{2+} in d_6-DMSO.

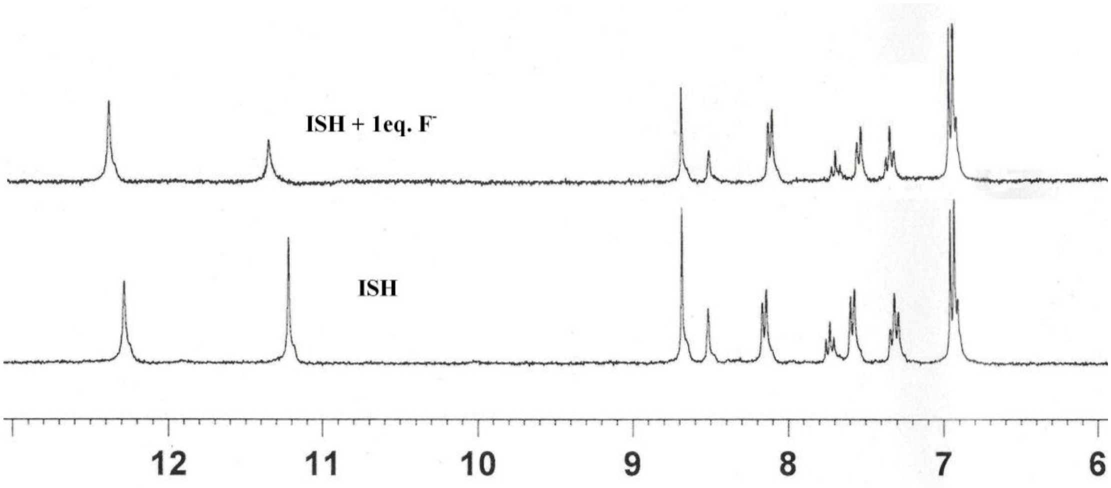

Figure S16: Partial ^{1}H-NMR spectra of ISH with addition of 1eq. F^- in d_6-DMSO.

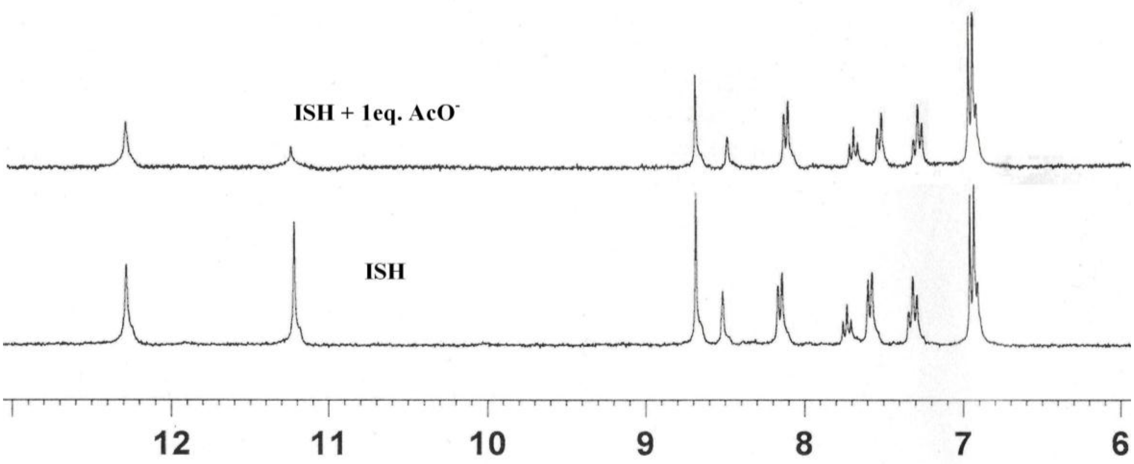

Figure S17: Partial ^{1}H-NMR spectra of ISH with addition of 1eq. AcO^- in d_6-DMSO.

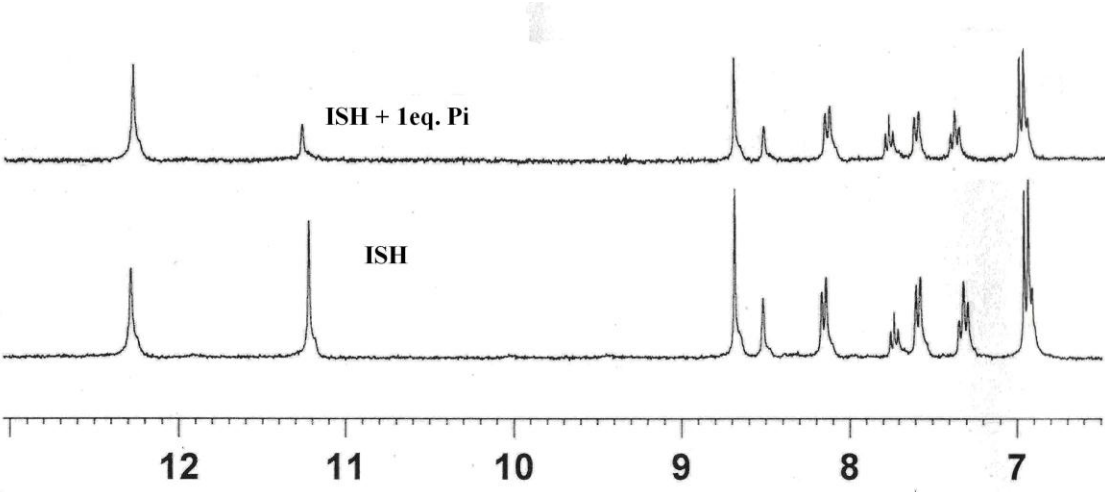

Figure S18: Partial [1]H-NMR spectra of ISH with addition of 1eq. Pi in d_6-DMSO.

7. Cyclic Voltammogram of ISH with addition of 2 eqiv. Al(III) and then 2 equiv. PPi.

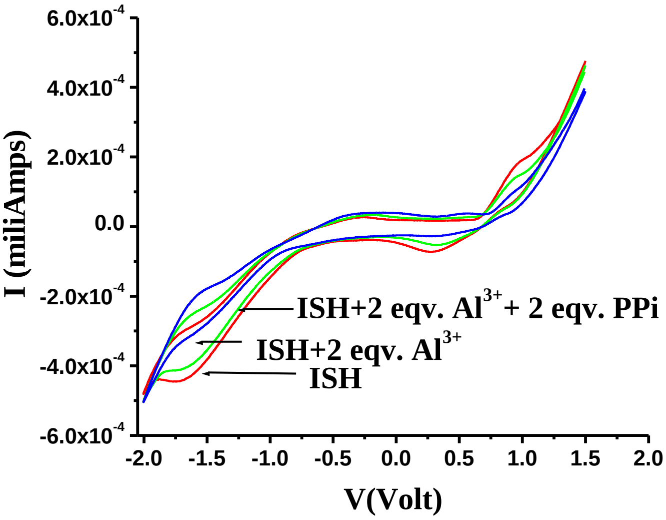

Figure S19: Cyclic Voltammogram of ISH with addition of Al(III) and PPi using $Hg/HgCl_2$ electrode in $MeOH/H_2O$ as a solvent.

8. Fluorescence emission spectra of ISH (C = 1x 10^{-5} M, in MeOH : H_2O (1:1, v/v) at pH 7.5) with different cations as Na^+, K^+, Ba^{2+}, Ga^{3+}, Mg^{2+}, Ca^{2+}, Mn^{2+}, Fe^{2+}, Ni^{2+}, Co^{2+}, Zn^{2+}, Cu^{2+}, Ag^+, Cd^{2+}, Hg^{2+}, Pb^{2+}, In^{3+}, $Cr^{3+}$and Fe^{3+} in MeOH : H_2O (C = 2x 10^{-4} M, 1:1, v/v). The solutions of metal ions were prepared from $NaClO_4$, $KClO_4$, $Ba(ClO_4)_2.4H_2O$, $GaCl_3$, $Mg(ClO_4)_2{\cdot}6H_2O$, $Ca(ClO_4)_2{\cdot}4H_2O$, $Mn(ClO_4)_2{\cdot}6H_2O$, $Fe(SO_4)_2$, $Ni(ClO_4)_2{\cdot}6H_2O$, $Co(ClO_4)_2{\cdot}6H_2O$, $Zn(ClO_4)_2{\cdot}6H_2O$, $Cu(ClO_4)_2{\cdot}6H_2O$, $AgNO_3$, $Cd(ClO_4)_2{\cdot}H_2O$, $HgCl_2$, $Pb(ClO_4)_2$, $InCl_3$, $CrCl_3.6H_2O$ and $FeCl_3$ respectively in MeOH-H_2O (1:1, v/v).

(a)

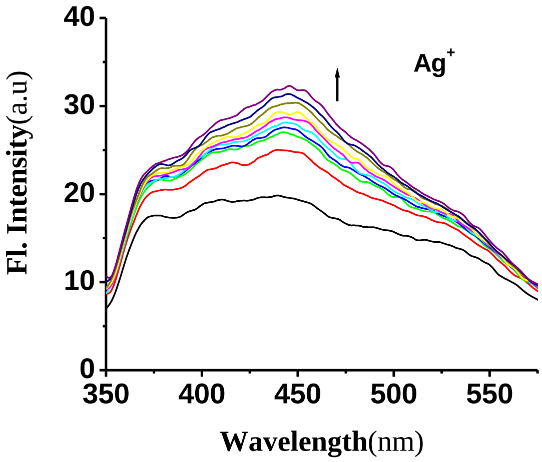
Ag+
Fl. Intensity(a.u)
Wavelength(nm)

(b)

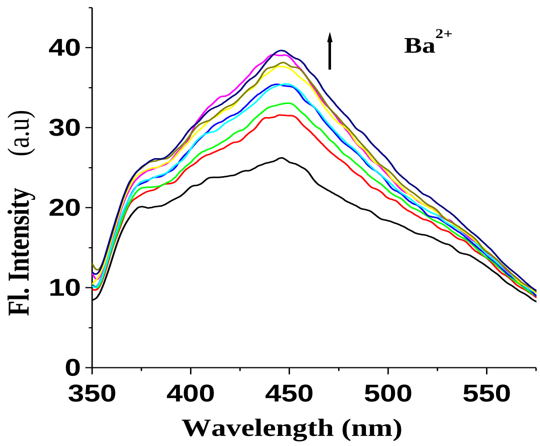
Ba2+
Fl. Intensity (a.u)
Wavelength (nm)

(c)

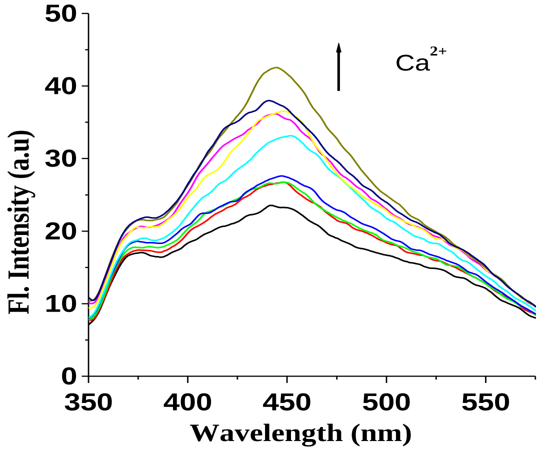
Ca2+
Fl. Intensity (a.u)
Wavelength (nm)

(d)

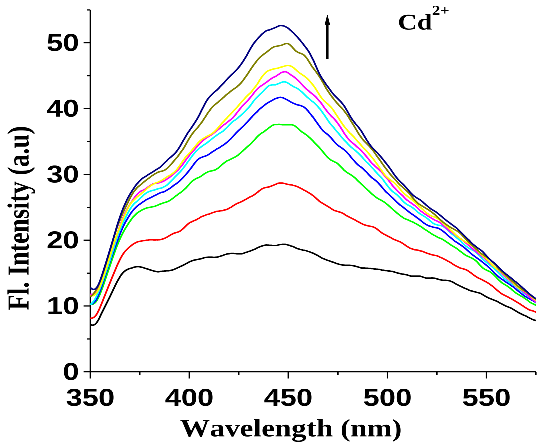
Cd2+
Fl. Intensity (a.u)
Wavelength (nm)

(e)

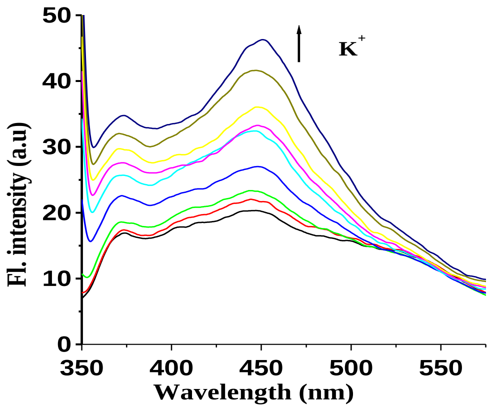
K+
Fl. intensity (a.u)
Wavelength (nm)

(f)

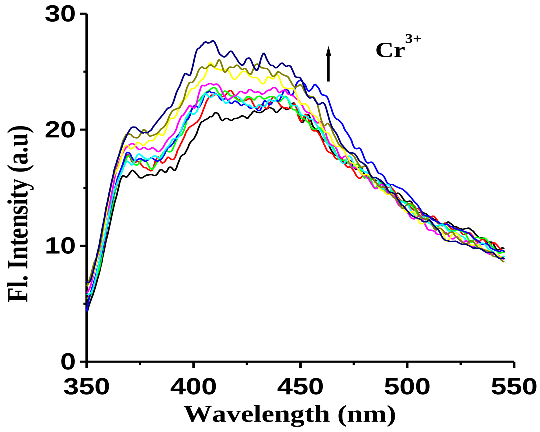
Cr3+
Fl. Intensity (a.u)
Wavelength (nm)

(g)

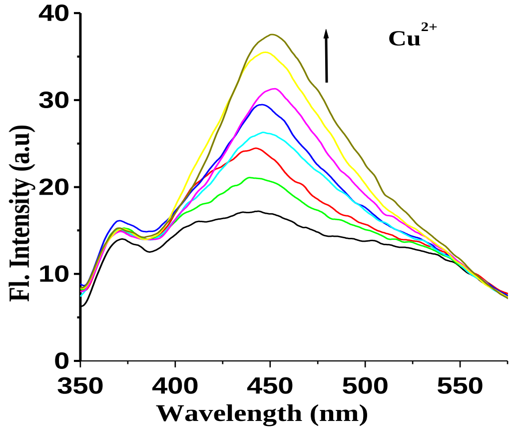
Cu2+
Fl. Intensity (a.u)
0
10
20
30
40
350
400
450
500
550
Wavelength (nm)

(h)

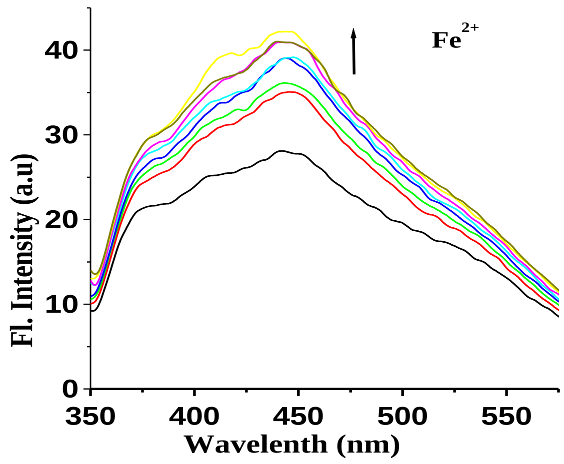
Fe2+
Fl. Intensity (a.u)
0
10
20
30
40
350
400
450
500
550
Wavelenth (nm)

(i)

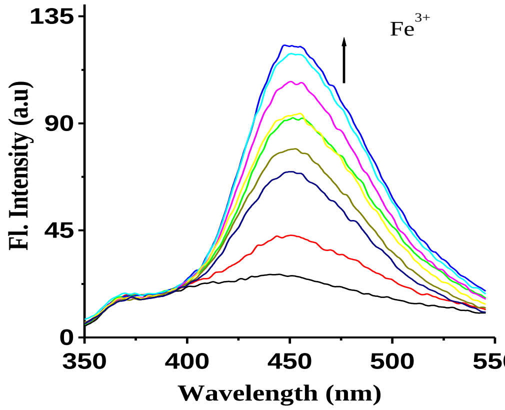
Fe3+
Fl. Intensity (a.u)
0
45
90
135
350
400
450
500
550
Wavelength (nm)

(j)

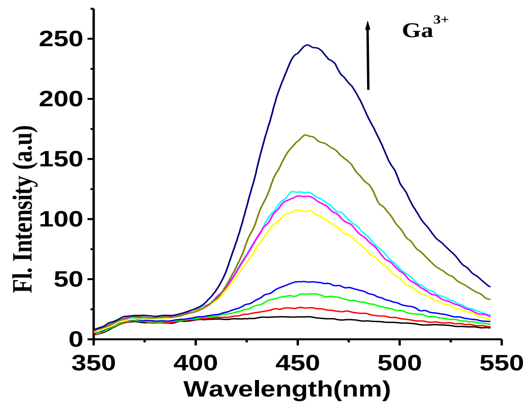
Ga3+
Fl. Intensity (a.u)
0
50
100
150
200
250
350
400
450
500
550
Wavelength(nm)

(k)

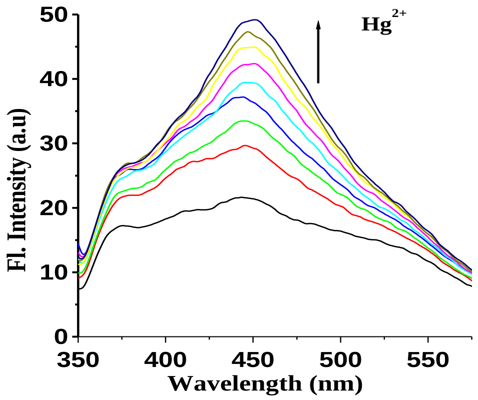
Hg2+
Fl. Intensity (a.u)
0
10
20
30
40
50
350
400
450
500
550
Wavelength (nm)

(l)

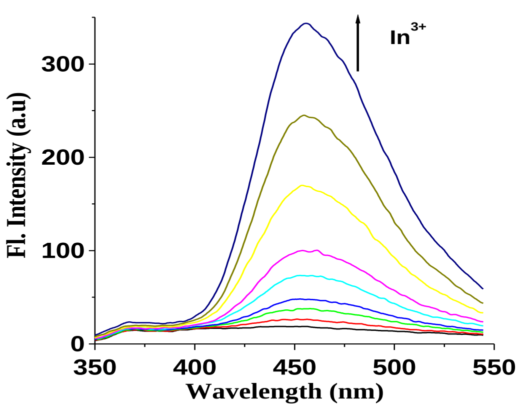
In3+
Fl. Intensity (a.u)
0
100
200
300
350
400
450
500
550
Wavelength (nm)

(m)

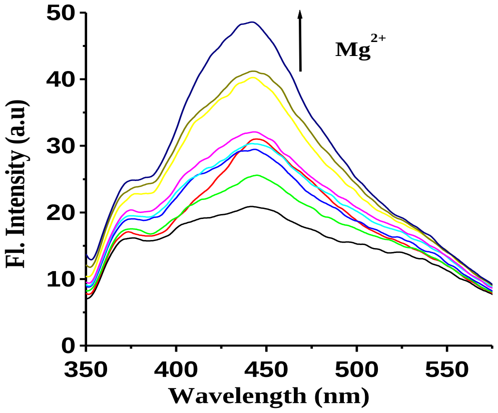
Mg2+
Fl. Intensity (a.u)
Wavelength (nm)
0
10
20
30
40
50
350
400
450
500
550

(n)

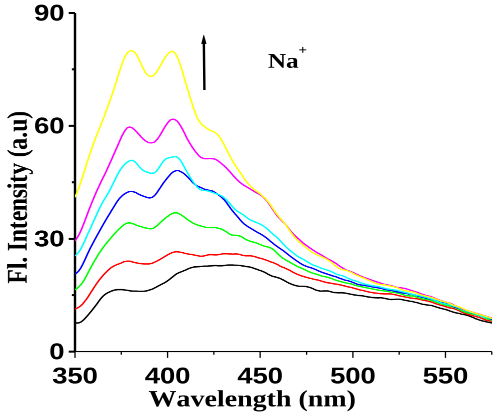
Na+
Fl. Intensity (a.u)
Wavelength (nm)
0
30
60
90
350
400
450
500
550

(o)

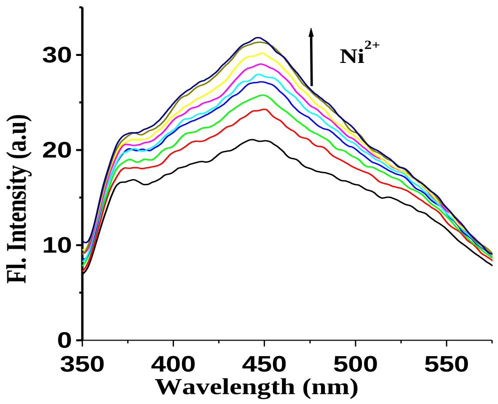
Ni2+
Fl. Intensity (a.u)
Wavelength (nm)
0
10
20
30
350
400
450
500
550

(p)

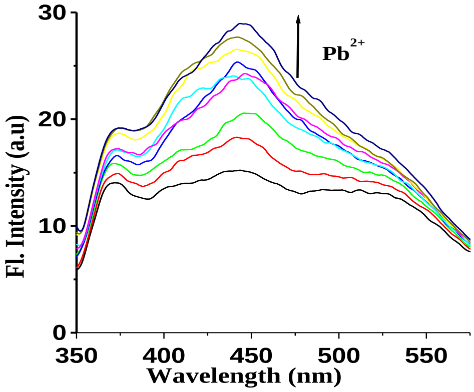
Pb2+
Fl. Intensity (a.u)
Wavelength (nm)
0
10
20
30
350
400
450
500
550

(q)

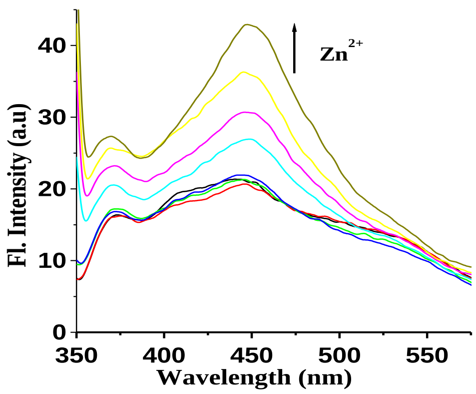
Zn2+
Fl. Intensity (a.u)
Wavelength (nm)
0
10
20
30
40
350
400
450
500
550

(r)

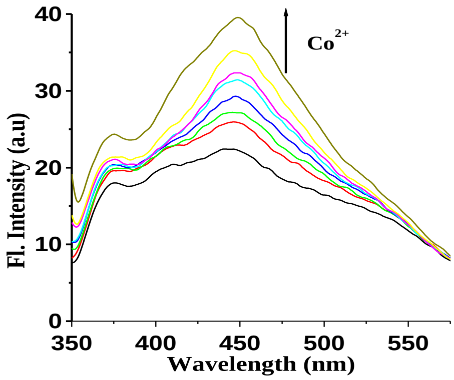
Co2+
Fl. Intensity (a.u)
Wavelength (nm)
0
10
20
30
40
350
400
450
500
550

(s)

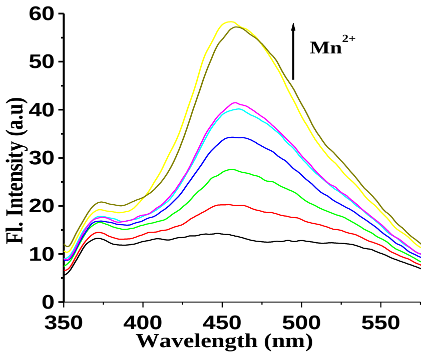

9. Fluorescence emission spectra of ISH (C = 1x 10^{-5} M, in MeOH : H_2O (1:1, v/v) at pH 7.5) with different anions as AcO^-, Cl^-, Br^-, I^-, F^-, BzO^-, SH^-, $H_2PO_4^-$, PO_4^{3-}, S^{2-}, N_3^-, ATP and ADP in MeOH : H_2O (C = 2x 10^{-4} M). The AcO^-, Cl^-, Br^-, I^-, F^- and BzO^- as their tetra butyl salts; SH^-, $H_2PO_4^-$, PO_4^{3-}, S^{2-}, N_3^-, $P_2O_7^{4-}$ and SCN^- as their sodium salts; ATP and ADP as their potassium salts in MeOH : H_2O solution (1:1, v/v).

(a)

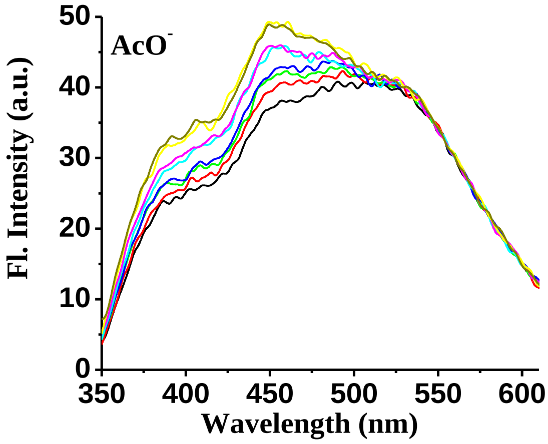

(b)

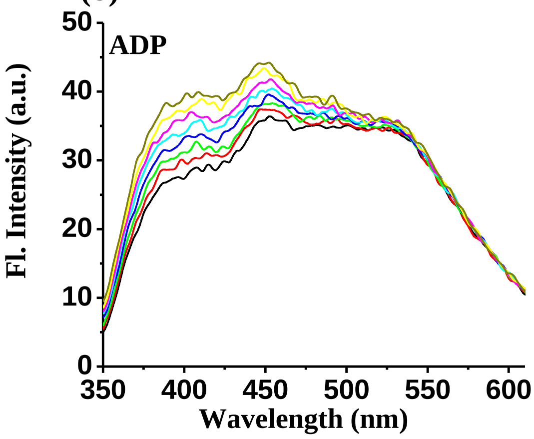

(c)

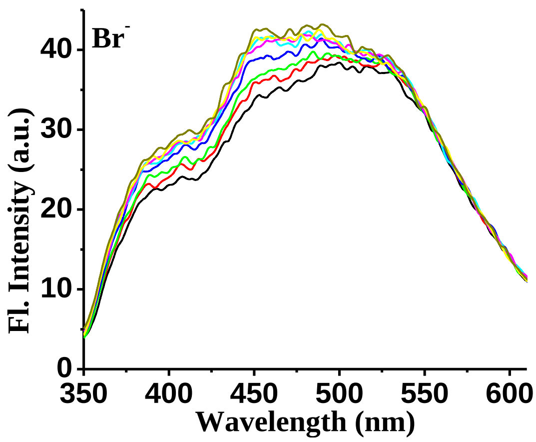

(d)

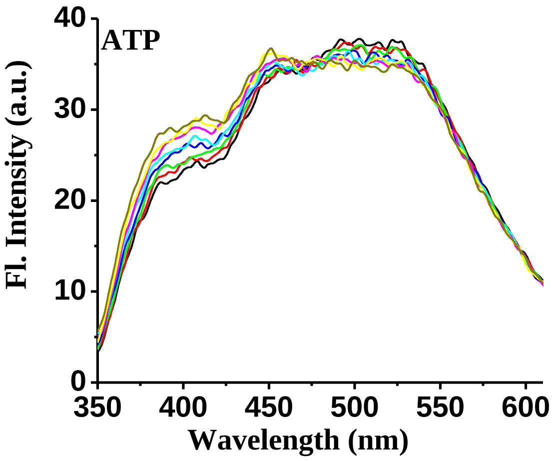

(e)

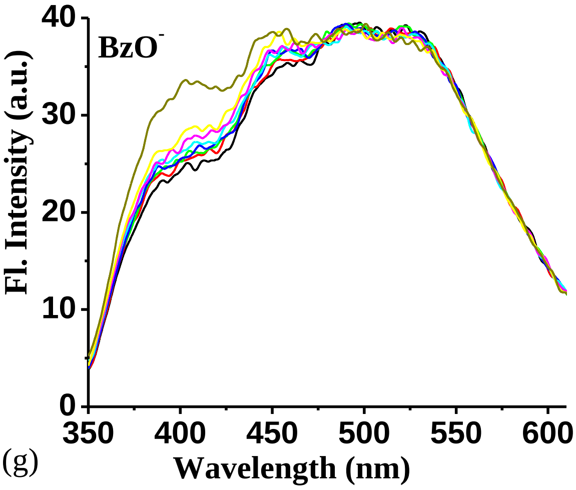
BzO-
Fl. Intensity (a.u.)
Wavelength (nm)

(f)

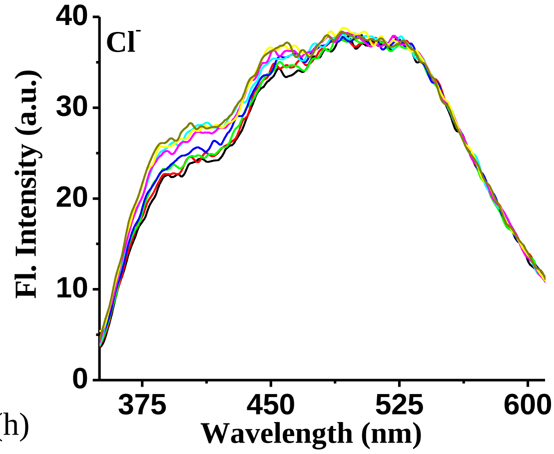
Cl-
Fl. Intensity (a.u.)
Wavelength (nm)

(g)

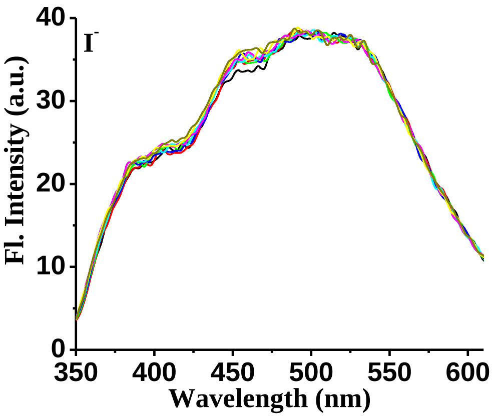
I-
Fl. Intensity (a.u.)
Wavelength (nm)

(h)

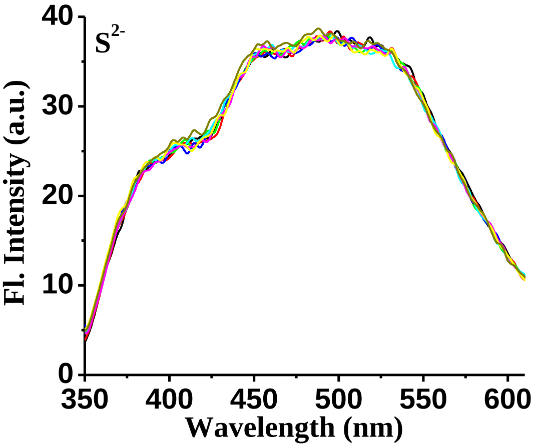
S2-
Fl. Intensity (a.u.)
Wavelength (nm)

(i)

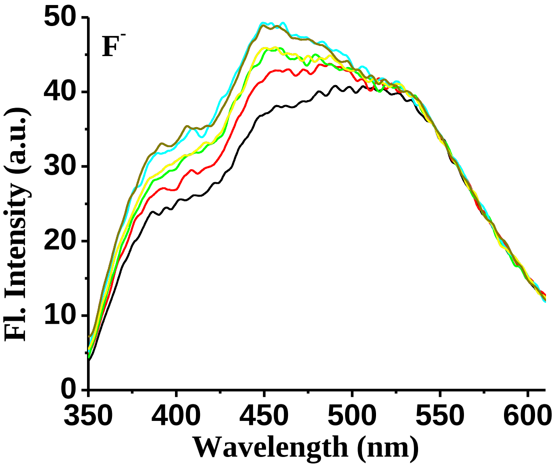
F-
Fl. Intensity (a.u.)
Wavelength (nm)

(j)

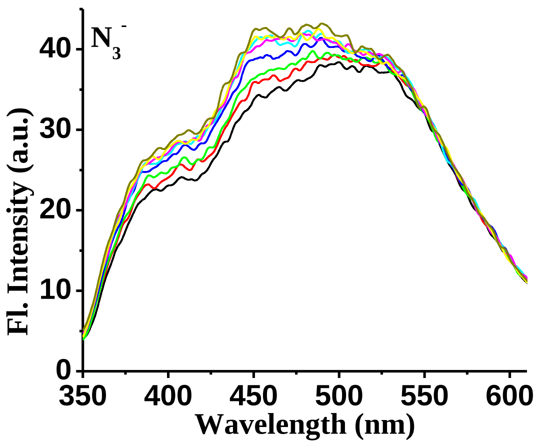
N3-
Fl. Intensity (a.u.)
Wavelength (nm)

(k)

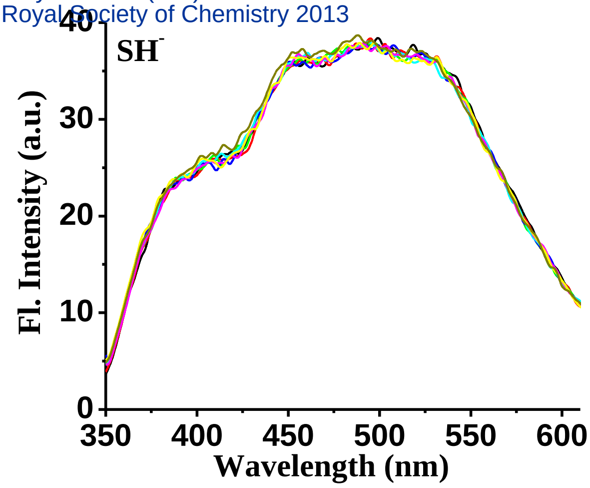

(l)

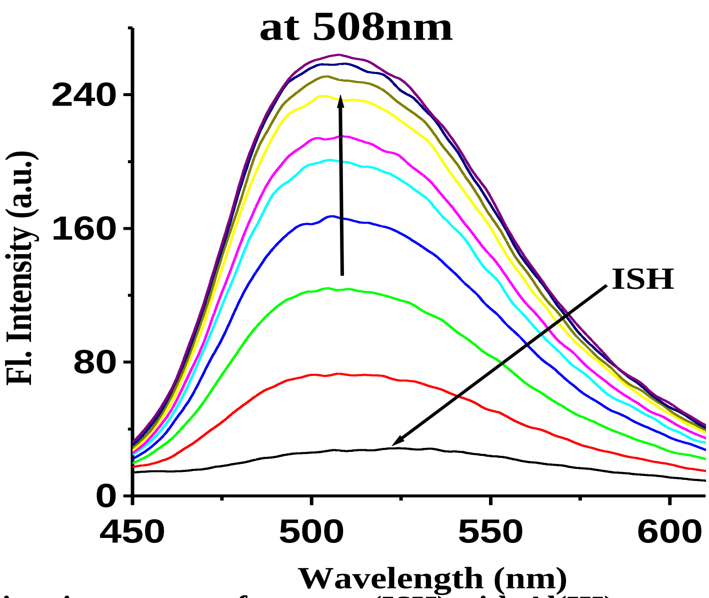

10. UV-*vis* titration spectra of receptor(ISH) with Al(III):

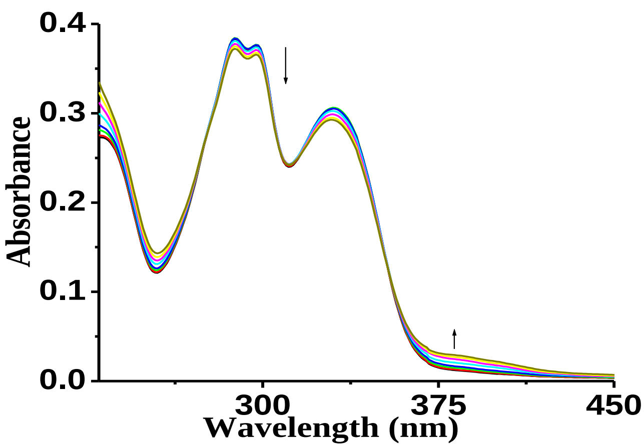

Figure S20: UV-Vis. titration spectra of ISH (c = 1.0 x 10^{-5} M) in presence of Al^{3+} (c = 2.0 x 10^{-4} M) at pH 7.5 in MeOH:H_2O = 1:1 (v/v).

11. FT-IR data of Receptor (above) and its complex with Al^{3+} ion (below):

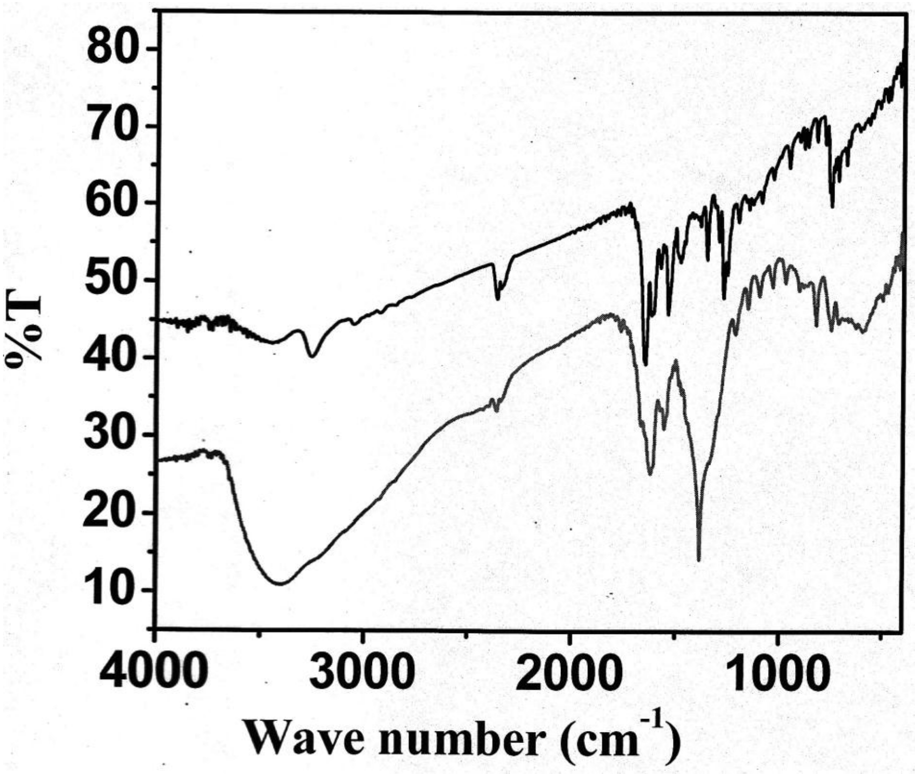

Figure S21: FT-IR spectra of ISH and its Al- complex.

12. References:

1. Valeur, B. Molecular *Fluorescence: Principles and Applications*. Wiley-VCH: Wenheim, 2002.
2. Zhu, M.; Yuan, M.; Liu, X.; Xu, J.; Lv, J.; Huang, C.; Liu, H.; Li, Y.; Wang, S.; Zhu, D. *Org. Lett.* 2008**,** *10*, 1481-1484.